scientific reports

Check for updates

OPEN

Metabolomics combined with metagenomics analysis reveals the potential mechanism of Zhejiang psyllium polysaccharides against hyperuricemia in rats

Dan Wu[1,5], Jingjie Niu[2,5], Jianping Hu[3], Hao Wang[1] & Haixue Kuang[4]✉

This study aimed to assess the anti-hyperuricemia efficacy of Zhejiang psyllium polysaccharides (ZPP) in rats and to explore its underlying mechanism. Hyperuricemia was induced by intragastric administration of potassium oxonate, hypoxanthine, and adenine. The serum levels of uric acid (UA), creatinine (Cr), and blood urea nitrogen (BUN) were measured, and kidney pathology was examined. Serum metabolomics was employed to monitor metabolic alterations following ZPP intervention. Metagenomic analysis was conducted to investigate the impact of ZPP on the intestinal flora of hyperuricemia rats. The results showed that ZPP could significantly reduce the serum UA level in hyperuricemia rats and exhibited a certain renal protective effect. The metabolomics results indicated that ZPP regulates uric acid levels in rats with hyperuricemia and ameliorates renal pathological changes by modulating biomarkers associated with purine metabolism, amino acid metabolism, and lipid metabolism. Metagenomic research also found that ZPP could increase the relative abundance of uric acid metabolism-related probiotics, such as *Limosilactobacillus reuteri* and *Lactobacillus murinus*, thereby improving intestinal flora imbalance in rats with hyperuricemia.

Keywords Zhejiang psyllium, Polysaccharide, Hyperuricemia, Metabolomics, Metagenomics

UA is the final oxidative product of purine catabolism. Sustained elevation of uric acid in the human body can lead to hyperuricemia[1]. Hyperuricemia is a metabolic disorder caused by disturbances in purine metabolism and is associated with various risk factors, which can trigger a series of complications such as gout, cardiovascular diseases, diabetes, and chronic kidney diseases[2,3]. Genetic factors, obesity, and lifestyle factors contribute to the prevalence of hyperuricemia[4–6]. Currently, the main treatments for hyperuricemia focus on inhibiting uric acid synthesis and promoting uric acid excretion[7]. However, drugs used in the process of lowering uric acid have varying degrees of side effects. For instance, the commonly used uric-lowering drugs allopurinol and benzbromarone have been restricted due to hepatotoxicity[8,9]. Increasingly, evidence shows that natural products contribute to the control of uric acid with low side effects, providing a new basis for safe and effective uric-lowering drug screening[10,11].

Metabolomics technology can identify metabolites with high throughput, analyze content changes, and complete the screening of differential metabolites in the course of disease[12]. This allows for the discovery of the pathological mechanisms of disease. Hyperuricemia, as a metabolic disorder, is usually accompanied by abnormal endogenous metabolites during its occurrence[13,14]. Recent studies have confirmed that metabolomics has been successfully applied to natural medicine in the mining of biomarkers and research on the mechanism of action related to the treatment or improvement of hyperuricemia[15,16]. Metabolomics will help us to understand the pathological process of hyperuricemia more deeply and may serve as a powerful tool to explore the mechanism of action of anti-hyperuricemia drugs.

[1]School of Medical, Quzhou College of Technology, Zhejiang 324000, China. [2]School of Chinese Materia Medica, Tianjin University of Chinese Medicine, Tianjin 301617, China. [3]Academician Workstation, Jiangxi University of Chinese Medicine, Jiangxi 330004, China. [4]Key Laboratory of Basicand Application Research of Beiyao, MinistryofEducation, Heilongjiang University of Chinese Medicine, Heilongjiang 150040, China. [5]Dan Wu and Jingjie Niu equally contributed to this work. ✉email: hxkuang@hljucm.edu.cn

The gut microbiota, composed of various microorganisms colonizing the human intestines, plays an irreplaceable role in regulating human metabolism. Structural changes or imbalances in the gut microbiota may lead to metabolic disorders within the organism[17,18]. Taking intestinal flora as the entry point to explore the pathogenesis of diseases has become a new research hotspot, especially in metabolic-related diseases such as hyperuricemia[19]. Genome-resolved metagenomics is a transformative approach in microbiome research, allowing for the analysis of the DNA of mixed microbial communities to assemble and directly analyze individual genomes from metagenomics data. This technology represents a significant advancement over traditional 16S rRNA sequencing, offering a rich depth of understanding and unprecedented insights into the microbiome[20]. The application of metagenomics technology to investigate the effect of drugs on hyperuricemia will provide new ideas for the mechanism studies.

Zhejiang psyllium is derived from the dried mature seeds of the *Plantago major* L., it is a plant belonging to the Plantain family. Along with the *Plantago asiatica* L. and the *Plantago depressa* Willd., Zhejiang psyllium is commercially available as Plantaginis Semen in China and is recorded in "Zhejiang Traditional Chinese Medicine Processing Norms (2015)"[21]. Zhejiang psyllium is rich in polysaccharides, and in addition, it also contains flavonoids, iridoids, phenylethanoid glycosides, and fatty acids[22–25]. Plantaginis Semen is often used as a diuretic medication and is widely applied in the treatment of hyperuricemia. In recent years, more and more studies have reported the preventive and therapeutic effects of Plantaginis Semen on hyperuricemia[26,27]. Plantaginis Semen polysaccharides can also reduce kidney inflammation and protect the kidney from damage in rats with gout nephropathy by regulating the expression of related proteins[28]. Despite these studies, further in-depth research is necessary to investigate the pharmacological effects of ZPP in improving hyperuricemia and its associated renal damage, and to elucidate the underlying mechanisms.

In this study, a hyperuricemic rat model was induced using potassium oxonate, hypoxanthine, and adenine to evaluate the therapeutic potential of ZPP. By employing integrated metabolomics and metagenomics approaches, the underlying mechanisms involving metabolic and microbial modulation in hyperuricemia were investigated. Consequently, this research aims to uncover novel approaches for the prevention and treatment of hyperuricemia.

Materials and methods

Reagents

Potassium oxonate (batch number: K2228616), hypoxanthine (batch number: E2224054), adenine (batch number: C2323028), benzbromarone (batch number: A2206687), and sodium carboxymethylcellulose (batch number: D2311614) were purchased from Shanghai Aladdin Biochemical Technology Co., Ltd. UA (batch number: 20231101), Cr (batch number: 20231105), and BUN (batch number: 20231213) reagent kits were purchased from Nanjing Jiancheng Bioengineering Institute Co., Ltd. Acetonitrile, methanol, and isopropanol were mass spectrometry grade. Anhydrous ethanol, petroleum ether, acetone, chloroform, and n-butanol were analytical grade. All the aforementioned chemical reagents were purchased from Shanghai Aladdin Biochemical Technology Co., Ltd.

Plant materials and preparation of ZPP

The seeds of Zhejiang psyllium were collected in Kaihua County, Quzhou City, and identified as the seeds of *Plantago major* L. by Song Jianfeng, the chief pharmacist of traditional Chinese medicine at Quzhou Institute for Food and Drug Control. The herbal specimen (No. 20221201) has been stored in the Herbarium of Quzhou College of Technology.

The dried seed was added to distilled water 10 times its weight for 3 times of decocting extraction (packet decocting), each lasting 2 h. After combining all the filtrates, the degreasing treatment was firstly conducted by using petroleum ether, and then degreased filtrate was concentrated. The concentrated liquid was redissolved in an appropriate amount of water, and 95% ethanol was slowly added while stirring until the ethanol concentration of the supernatant reached 85%. This mixture was allowed to stand at 4 °C for 24 h, and then it was centrifuged at 1200 × g for 20 min to obtain the precipitate. This ethanol precipitation process was repeated three times, with the supernatants and precipitates from each time being combined separately. The precipitate obtained from the three ethanol precipitations was dried and washed alternately with anhydrous ethanol and acetone. The washed precipitate was redissolved in distilled water (at a ratio of 0.5 g of crude drug per mL). The chloroform and n-butanol mixed solution was added to the solution, and it was shaken vigorously to remove proteins. It was centrifuged again at 1200 × g for 20 min, the supernatant was taken, concentrated, and dried, and finally the ZPP fraction was obtained.

Animals and drug administration

Male Sprague Dawley rats, aged 8 weeks and weighing (200 ± 20) g, were purchased from Beijing Vital River Laboratory Animal Technology Co., Ltd., with an animal license number of SCXK(Jing)2021–0006. The animal room was maintained at a temperature of 24 ± 2 °C, with a 12-h light–dark cycle, relative humidity of 45 ± 5%, and clean air circulation. The feed and distilled water were sterile-processed, and the rats were acclimated for one week before the experiment.

Rats were randomly divided into six groups(8 rats in each group): control group, hyperuricemia model group, benzbromarone group, low-dose ZPP group (400 mg/kg), medium-dose ZPP group (800 mg/kg), and high-dose ZPP group (1600 mg/kg). Except for the normal control group, all other groups were established as hyperuricemia models by administering a combination of potassium oxonate, hypoxanthine, and adenine. Potassium oxonate (200 mg/kg), hypoxanthine (500 mg/kg), and adenine (50 mg/kg) were mixed in 0.5% sodium carboxymethylcellulose to prepare a suspension. The modeling was conducted by continuous gavage

administration for 21 days. The drug administration was performed 2 h after modeling and continued by gavage for another 21 days.

Sample collection and preparation

After 21 days of modeling and drug administration, the experimental rats were fasted for 12 h before euthanasia with free access to water. Before anesthesia, under sterile conditions, five feces pellets were collected from each experimental rat and temporarily stored on dry ice. Within 2 h, the feces were transferred to sterile, pyrogen-free Eppendorf tubes for metagenomics analysis. After an intraperitoneal injection of pentobarbital sodium for anesthesia, blood was collected from the abdominal aorta, and the rats were immediately euthanized via intravenous injection of pentobarbital sodium. Promptly extract the left kidney and place it in 4% paraformaldehyde for fixation, intended for subsequent pathological observation, while the right kidney tissue was temporarily stored in liquid nitrogen. The collected blood was allowed to sit for 1 h and then centrifuged at 900 × g for 10 min. The supernatant (serum) was collected and aliquoted into sterile, pyrogen-free Eppendorf tubes. The levels of UA, Cr, and BUN in the serum were measured according to the manufacturer's instructions provided with the assay kits. In serum metabolomics research, 100 µL of serum samples were thawed at 4 °C before analysis. Serum proteins were precipitated with 300 µL of acetonitrile and subsequently removed by centrifugation at 17,000 × g for 10 min. The supernatant was dried under nitrogen at 30 °C and then redissolved in 100 µL of acetonitrile/water (80:20, v/v). Each resuspended sample was centrifuged at 17,000 × g for 10 min, and the supernatant was transferred to injection vials for metabolomics analysis.

All methods were carried out in accordance with ARRIVE guidelines and ethical regulations for animal experimentation of Tianjin University of Chinese Medicine.

Renal histopathological observation

After fixation with 4% paraformaldehyde, the kidney undergoes precise trimming, dehydration, embedding, sectioning, staining with hematoxylin–eosin (HE), and mounting, following the standard operating procedure (SOP) for pathological experiments. Subsequently, the sections were carefully examined under a microscope, with details of the tissue sections observed at a magnification of 200 ×.

UPLC-Q-TOF/MS instrument conditions

Chromatographic separation was performed using a UPLC system with an ACQUITY UPLC HSS T3 column (100 mm × 2.1 mm, 1.8 µm). The injection volume was 2 µL; the flow rate was 0.3 mL/min; and the column temperature was maintained at 40 °C. Mobile phase A consisted of water with 0.1% formic acid, while mobile phase B was acetonitrile with 0.1% formic acid. The gradient elution conditions were as follows: 0 ~ 0.5 min, 95% A; 0.5 ~ 9 min, 95% ~ 40% A; 9 ~ 12 min, 40% ~ 2% A; 12 ~ 17 min, 2% A; 17 ~ 17.1 min, 2% ~ 95% A; 17.1 ~ 20 min, 95% A.

The ESI ion source was selected in both positive and negative ion modes, with Information-Dependent Acquisition (IDA) as the scan mode. The ion spray voltage was set at + 5500/-4500 V, the nebulizer gas flow rate was 50 psi, the desolvation gas flow rate was 55 psi, and the curtain gas flow rate was 35 psi. For TOF MS conditions, the mass scan range was set from m/z 70 to 1300 Da, with a collection time of 0.25 s, a declustering potential of ± 80V, and a collision energy of ± 10V.

Metabolomics analysis

Samples were analyzed using UPLC-Q-TOF/MS technology to obtain data, which were then imported into the Progenesis QI software v2.1 (Nonlinear Dynamics, Newcastle upon Tyne, UK) workstation for preprocessing steps including peak matching, noise filtering, peak area normalization, and scaling. The preprocessed data were uploaded to the EZinfo 3.0 (Nonlinear Dynamics, Newcastle upon Tyne, UK) and SIMCA 14.1 (Umetrics AB, Umea, Sweden) software for multivariate statistical analysis. Partial Least Squares Discriminant Analysis (PLS-DA) was employed for multi-group comparisons to deeply explore potential information and classification differences within the data. Permutation tests were used to verify the validity of the PLS-DA model. Significant differential metabolites were screened based on the criteria of Variable Importance for the Projection (VIP) > 1 and p-value < 0.05. The selected differential metabolites were structurally identified using the Human Metabolome Database (HMDB) based on scored ≥ 30 (The score given to the compound identification by the search engine used to provide it) and mass error ≤ 10 ppm (The difference between theoretical and measured mass, expressed in parts per million). Pathway enrichment analysis was conducted using the Kyoto Encyclopedia of Genes and Genomes (KEGG) database (http://www.kegg.jp/kegg/kegg1.html) and the MetaAnalyst platform (http://www.metaanalyst.ca)[29,30].

Metagenomics analysis

Genomic DNA was extracted from fecal samples using the CTAB method and the extracted genomic DNA was detected using 1% agarose gel electrophoresis. The instrument Covaris M220 was used to fragment the DNA to a size of 350 bp. A PE library was constructed by attaching specific adapters to both ends of the DNA fragments, and magnetic beads were used to screen and remove adapter-self-ligated fragments. PCR amplification was performed to enrich the library template, followed by sodium hydroxide denaturation to produce single-stranded DNA fragments. Bridge PCR was conducted to amplify the DNA molecules, ensuring high efficiency and accuracy during sequencing. Illumina sequencing was performed as required, and the sequence of the template DNA fragments was determined by collecting the fluorescence signals in each cycle. For data analysis, the raw sequences were first optimized through splitting, quality trimming, and contamination removal. The optimized sequences were then used for assembly and gene prediction. The obtained genes were annotated and classified in terms of species and function to obtain valid data for subsequent analysis.

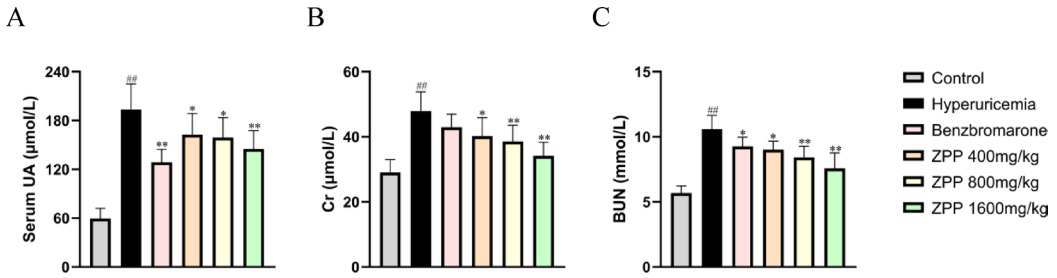

Fig. 1. Effect of ZPP on Serum (**A**) UA level, (**B**) Cr level, (**C**) BUN level. All values are mean ± standard deviation(n = 8). $^{\#}p < 0.05$ and $^{\#\#}p < 0.01$ compared with the Control group. $^{*}p < 0.05$ and $^{**}p < 0.01$ compared with the hyperuricemia group.

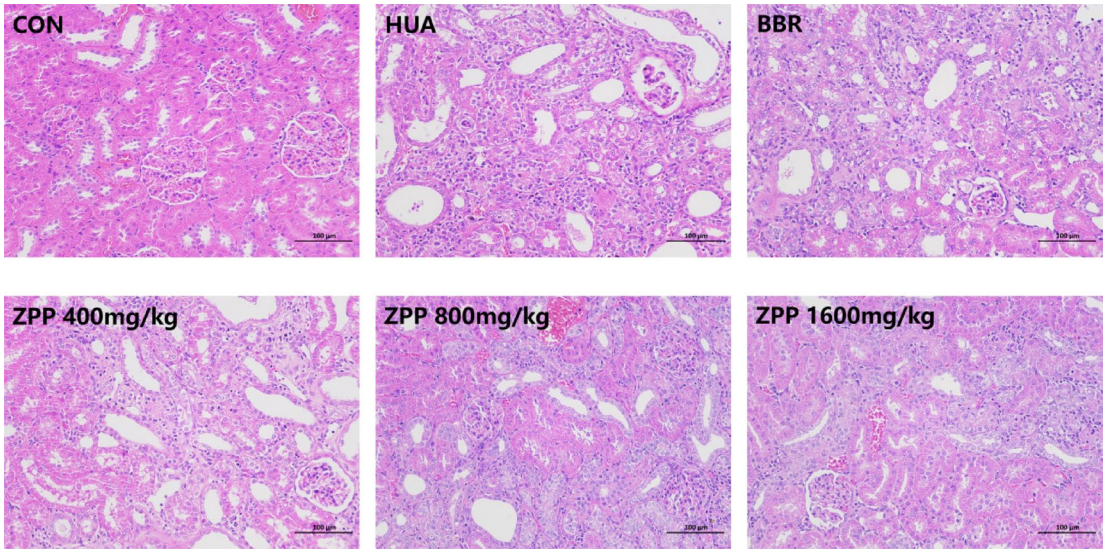

Fig. 2. Representative H&E stained sections of rat kidney. Scale bar = 100 μm, original magnification 200×.

Statistical analysis

Experimental data were analyzed using GraphPad Prism 10 software (GraphPad Software, San Diego, CA, USA) to perform one-way analysis of variance (ANOVA) and Dunnett's multiple comparisons test. The results are presented as mean ± standard deviation (SD).

Results

Effects of ZPP on serum UA, Cr, and BUN levels

By comparing the serum uric acid levels in rats from the hyperuricemia (HUA) group with those from the control (CON) group, the results showed that the UA levels in the HUA group were significantly higher than those in the CON group ($p < 0.01$), confirming the successful establishment of the hyperuricemia model. Additionally, the levels of Cr and BUN in the serum of rats in the HUA group were also significantly elevated ($p < 0.01$, $p < 0.01$), indicating that the model rats exhibited notable hyperuricemia accompanied by renal function impairment. Further experimental findings confirmed that ZPP exhibits a capacity to lower serum UA levels in rats suffering from hyperuricemia ($p < 0.05$, $p < 0.05$, and $p < 0.01$), regardless of whether administered at low, medium, or high doses (Fig. 1A). Compared with the HUA group, the levels of Cr ($p < 0.05$, $p < 0.01$, and $p < 0.01$) and BUN ($p < 0.05$, $p < 0.01$, and $p < 0.01$) in rats from all ZPP dose groups were significantly decreased (Fig. 1B,C). These findings suggested that ZPP has a therapeutic effect on hyperuricemia to a certain extent and can improve renal function indicators.

Effects of ZPP on kidney injury caused by hyperuricemia

In the renal tissue of rats in the control group, the number of cells in the glomeruli was normal, and the matrix was uniform. The renal tubular epithelial cells were round and full, with neatly arranged and regular brush borders. There was no significant interstitial hyperplasia, and no obvious inflammatory cell infiltration was observed (Fig. 2). In contrast, the renal tissue of rats in the model group exhibited pathological symptoms such as renal tubular dilation, edema of renal tubular epithelial cells, and interstitial connective tissue hyperplasia, accompanied by inflammatory cell infiltration dominated by lymphocytes (Fig. 2). Notably, the degree of

renal tissue pathology was improved in rats from all ZPP dosage groups, with a significant reduction in renal tubular dilation and epithelial cell edema. The interstitial connective tissue hyperplasia was inhibited, and the inflammatory cell infiltration was markedly decreased (Fig. 2).

Effects of ZPP on endogenous metabolites

Partial Least Squares Discriminant Analysis (PLS-DA) is a discriminant analysis technique within multivariate data analysis. By employing PLS-DA to analyze the differences in metabolite expression profiles among the blank CON group, HUA group, and ZPP intervention group, the aim is to explore the pathological mechanisms of hyperuricemia and identify potential biomarkers for the response to ZPP. The PLS-DA score plot visually demonstrates a clear distinction among the three groups of samples under both positive and negative ion detection modes, validating the reliability of the hyperuricemia rat model and the effectiveness of ZPP in modulating hyperuricemia serum metabolism (Fig. 3A,B). Further permutation test analysis reveals that the model exhibits high explanatory power ($R^2Y = 0.987$) and predictive accuracy ($Q^2 = 0.865$) in the positive ion mode, while maintaining good performance ($R^2Y = 0.978$, $Q^2 = 0.826$) in the negative ion mode (Fig. 3C,D). These results fully demonstrate the robust capability of the PLS-DA model in handling complex biological data and the robustness of the research conclusions, laying a solid foundation for subsequent biomarker discovery and drug efficacy evaluation.

In both positive and negative ion modes, based on PLS-DA analysis of different metabolites in each group, differential metabolites that met the criteria of VIP (Variable Importance in Projection) > 1 (Fig. 3E,F) and $p < 0.05$ were screened out. A total of 23 potential endogenous biomarkers were identified through the HMDB database (Table 1). The quantitative changes of these biomarkers were presented in the form of a heatmap (Fig. 4).

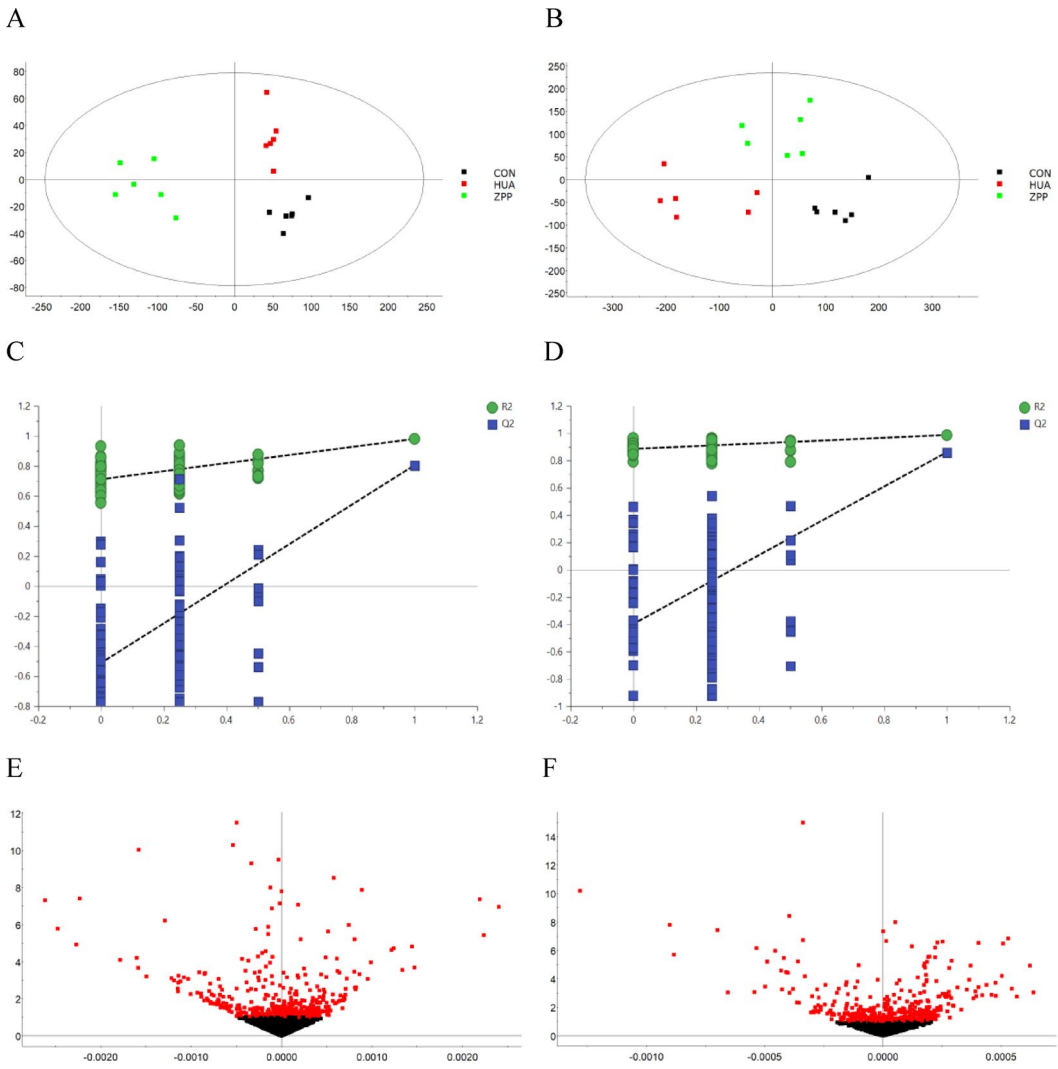

Fig. 3. Metabolomics analyses of serum samples. (**A**, **B**) PLS-DA score plots of the three groups from the CON, the HUA, and the ZPP group in positive mode and negative mode. (**C**, **D**) Permutation test from the model and the drug-treated group in positive mode and negative mode. (**E, F**) VIP plots for PLS-DA models in positive mode and negative mode. The red dot means VIP > 1.0.

NO	Ionization method	Metabolite	m/z	Molecular formula	*p*	VIP	CON vs. HUA	HUA vs. ZPP
1	ESI +	Cholesterol	369.3511	$C_{27}H_{46}O$	2.05×10^{-4}	1.47	↓	↑
2	ESI –	Deoxyinosine	287.0525	$C_{10}H_{12}N_4O_4$	5.76×10^{-3}	2.46	↓	↑
3	ESI –	Lactic acid	89.0240	$C_3H_6O_3$	$1.66\times10^{-}2$	1.41	↑	↓
4	ESI –	Palmitic acid	255.2323	$C_{16}H_{32}O_2$	3.18×10^{-4}	7.80	↓	↑
5	ESI +	Sphinganine	302.3050	$C_{18}H_{39}NO_2$	2.29×10^{-4}	1.52	↑	↓
6	ESI –	Sphingosine 1-phosphate	378.2416	$C_{18}H_{38}NO_5P$	$1.99\times10^{-}2$	3.56	↑	↓
7	ESI –	Xanthosine	283.0687	$C_{10}H_{12}N_4O_6$	2.49×10^{-3}	2.88	↓	↑
8	ESI +	Arginine	175.1190	$C_6H_{14}N_4O_2$	1.05×10^{-4}	1.58	↓	↑
9	ESI +	Glutamine	169.0582	$C_5H_{10}N_2O_3$	2.09×10^{-4}	2.88	↓	↑
10	ESI –	Hydroxypropionic acid	89.0241	$C_3H_6O_3$	1.59×10^{-2}	3.19	↑	↓
11	ESI +	Indoleacrylic acid	205.0884	$C_{11}H_9NO_2$	3.88×10^{-3}	2.99	↑	↓
12	ESI –	Stearic acid	283.2638	$C_{18}H_{36}O_2$	1.86×10^{-3}	3.80	↑	↓
13	ESI –	Arachidonic acid	303.2321	$C_{20}H_{32}O_2$	2.73×10^{-2}	4.94	↓	↑
14	ESI +	Deoxyuridine triphosphate	490.9643	$C_9H_{15}N_2O_{14}P_3$	6.41×10^{-6}	2.04	↓	↑
15	ESI +	Allantoic acid	177.0612	$C_4H_8N_4O_4$	6.91×10^{-4}	3.82	↓	↑
16	ESI +	Theophylline	203.0526	$C_7H_8N_4O_2$	2.84×10^{-5}	5.17	↑	↓
17	ESI –	Eicosapentaenoic acid	301.2177	$C_{20}H_{30}O_2$	2.93×10^{-2}	1.12	↑	↓
18	ESI –	12-Keto-tetrahydro-leukotriene B4	337.2364	$C_{20}H_{34}O_4$	3.64×10^{-3}	1.55	↓	↑
19	ESI –	Estrone glucuronide	445.1907	$C_{24}H_{30}O_8$	2.51×10^{-2}	1.76	↓	↑
20	ESI +	CE(20:4)	690.6200	$C_{47}H_{76}O_2$	2.11×10^{-3}	2.77	↑	↓
21	ESI +	LysoPC(18:1)	522.3546	$C_{26}H_{52}NO_7P$	3.62×10^{-4}	5.78	↑	↓
22	ESI +	LysoPC(20:4)	544.3394	$C_{28}H_{50}NO_7P$	4.37×10^{-4}	1.78	↑	↓
23	ESI –	LysoPE(18:0)	480.3096	$C_{23}H_{48}NO_7P$	5.38×10^{-4}	4.95	↑	↓

Table 1. 23 identified regulated metabolites from ZPP using UPLC-Q-TOF/MS.

Effects of ZPP on the metabolic pathway of potential biomarkers

To evaluate the therapeutic effect of ZPP on hyperuricemia in rats and elucidate its mechanism of action, we investigated the response of perturbed differential metabolites following ZPP treatment after model establishment. The HMDB or KEGG IDs of the 23 identified regulated metabolites from ZPP were imported into the MetaboAnalyst 6.0 platform for metabolic pathway analysis, and potential metabolic pathways were screened based on $p < 0.05$ or Impact > 0 (Table S1). The metabolic pathways involved in hyperuricemia include biosynthesis of unsaturated fatty acids, purine metabolism, arginine biosynthesis, sphingolipid metabolism, steroid biosynthesis, arachidonic acid metabolism, alanine, aspartate, and glutamate metabolism, as well as arginine and proline metabolism (Fig. 5).

Effects of ZPP on the structural dysregulation of the intestinal flora

Metagenomics relies on high-throughput sequencing of species' gene sequences, enabling detailed focus on the species level of the gut microbiota. Based on the gene sequences and relative abundances obtained through sequencing, species annotation was conducted for the gut microbiota of rats in each group. At the phylum level, Firmicutes, Bacteroidetes, unclassified_d__Bacteria, Actinobacteria, Candidatus_Saccharibacteria, Proteobacteria, and Uroviricota were identified (Fig. 6A). Among them, Firmicutes and Bacteroidetes were the dominant phyla. When compared to both the CON group and the ZPP group, the model group showed a higher relative abundance of Bacteroidetes and a lower relative abundance of Firmicutes. The results suggested that ZPP can regulate the composition and structure of the gut microbiota in HUA rats to a certain extent. At the species level, compared to both the control group and the ZPP group, the model group exhibited decreased relative abundances of *Lachnospiraceae_bacterium*, *Oscillospiraceae_bacterium*, *Limosilactobacillus_reuteri*, *Ligilactobacillus_murinus*, *Eubacterium_sp.*, and *Bacilli_bacterium* (Fig. 6B). Corresponding to these results, the clustering plot of PCoA showed that the clustering of the model group was distant from the control group, while after ZPP intervention, the clustering tended to normalize (Fig. 6C).

Effects of ZPP on the function of the gut microbiota

Linear Discriminant Analysis (LDA) estimated the abundance of each species in terms of taxonomic differences. To screen out microorganisms with biological significance among different experimental groups from the vast amount of gut microbiota data, and to assess their variability and effect sizes across groups, we conducted LDA Effect Size (LEfSe) analysis, estimating the magnitude of impact each species had on the differential effects (Fig. 7A). The LDA results showed that, in the HUA group, the more differentiated bacterial genera were Eggerthellales order, Eggerthellaceae family, and Peptostreptococcaceae family. In the ZPP group, the more differentiated bacterial genera were Eubacteriales order, Clostridia class, and Firmicutes phylum (Fig. 7B).

The Circos plot for samples and species functions provides a clear depiction of the correspondence between sample abundance and species functions. The results indicate that ZPP primarily affects metabolic pathways such

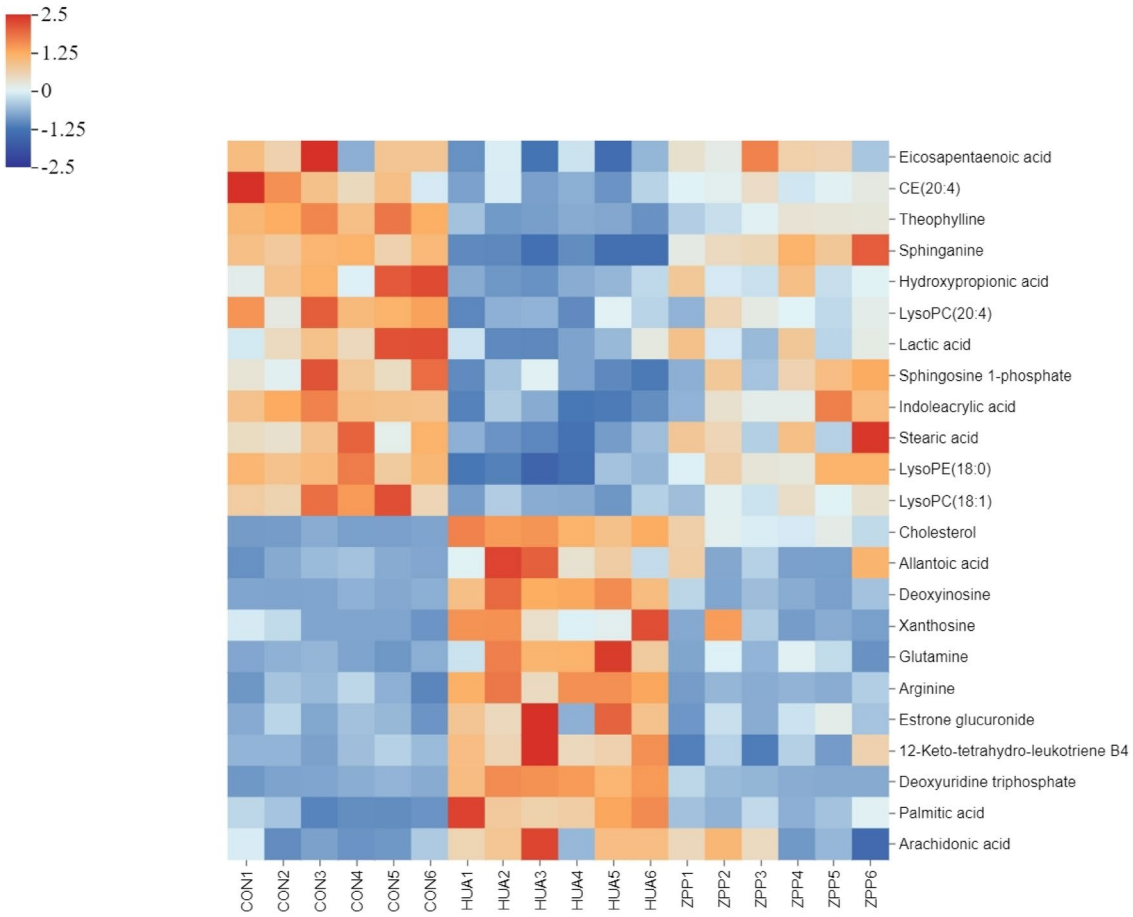

Fig. 4. Hierarchical clustering heat map of the 23 differential metabolites, with the degree of change marked in red (up-regulation) and blue (down-regulation).

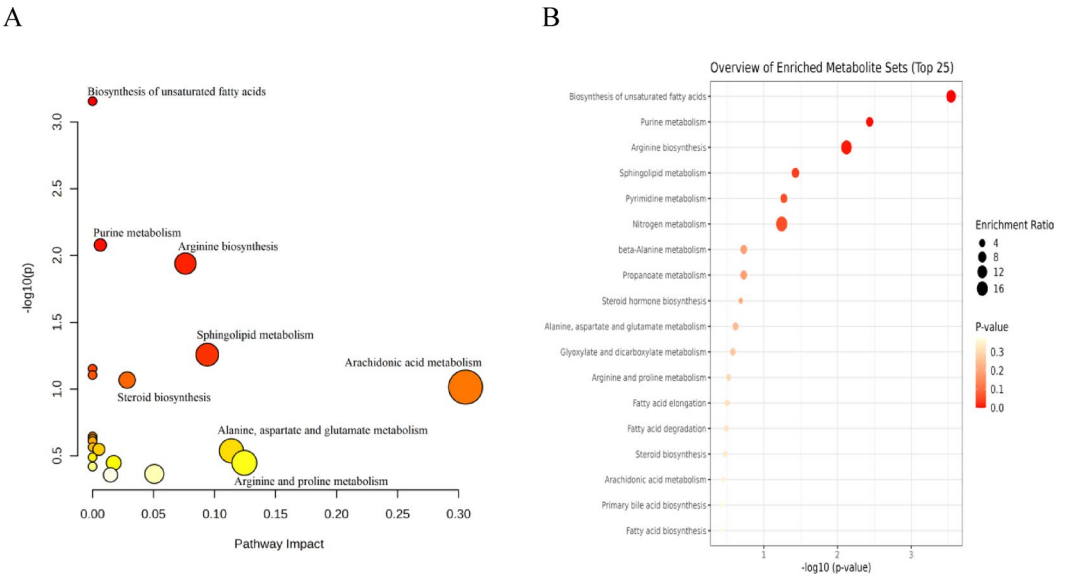

Fig. 5. Pathway analysis (**A**) and enrichment analysis (**B**) of potential biomarkers affected by ZPP.

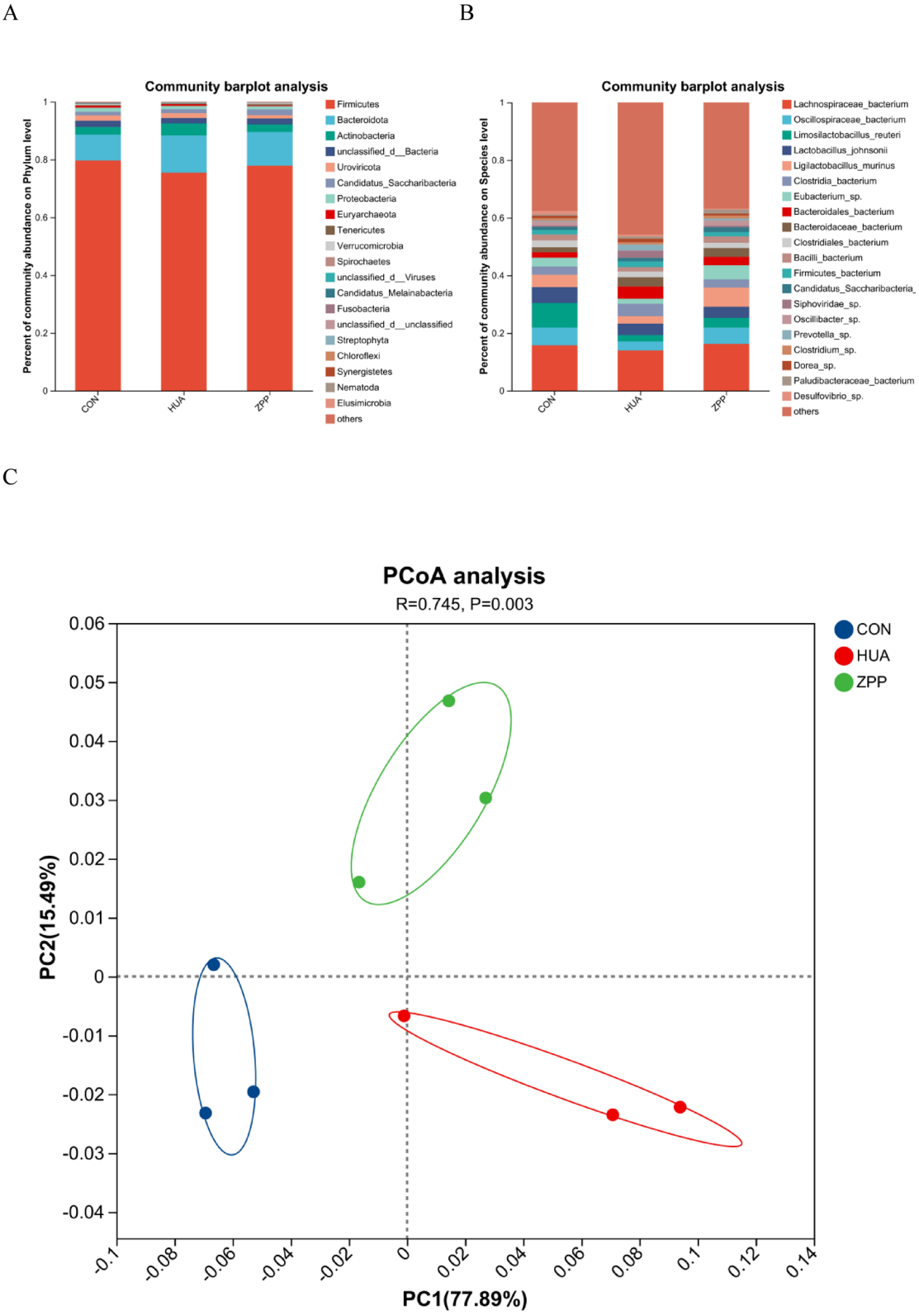

Fig. 6. Metagenomics reveals differences in microbial (**A**) phylum-level and (**B**) species-level composition in hyperuricemia rats after ZPP intervention. (**C**) PcoA analysis of each group.

A

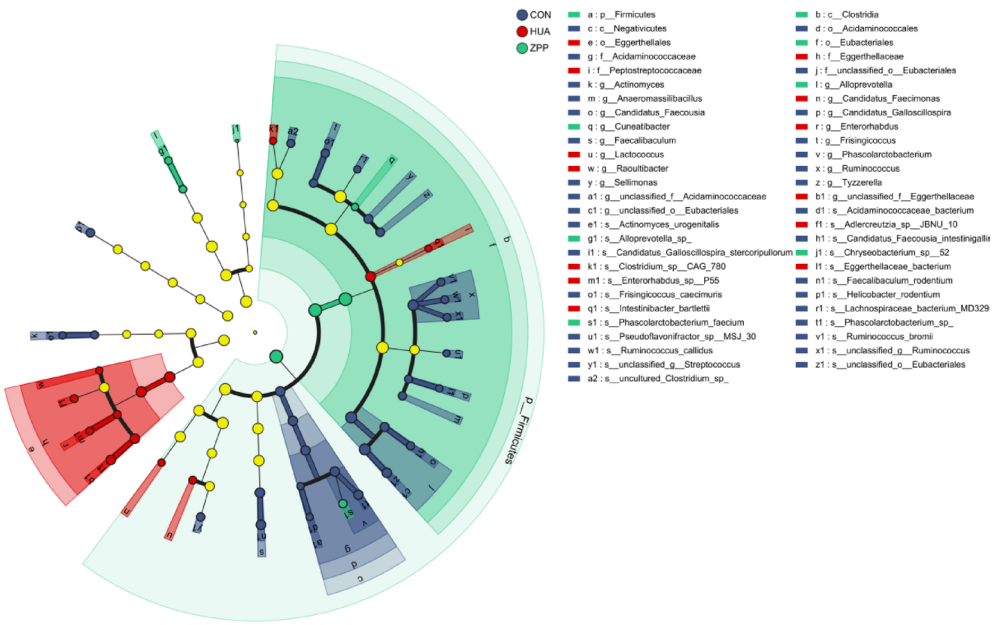

B

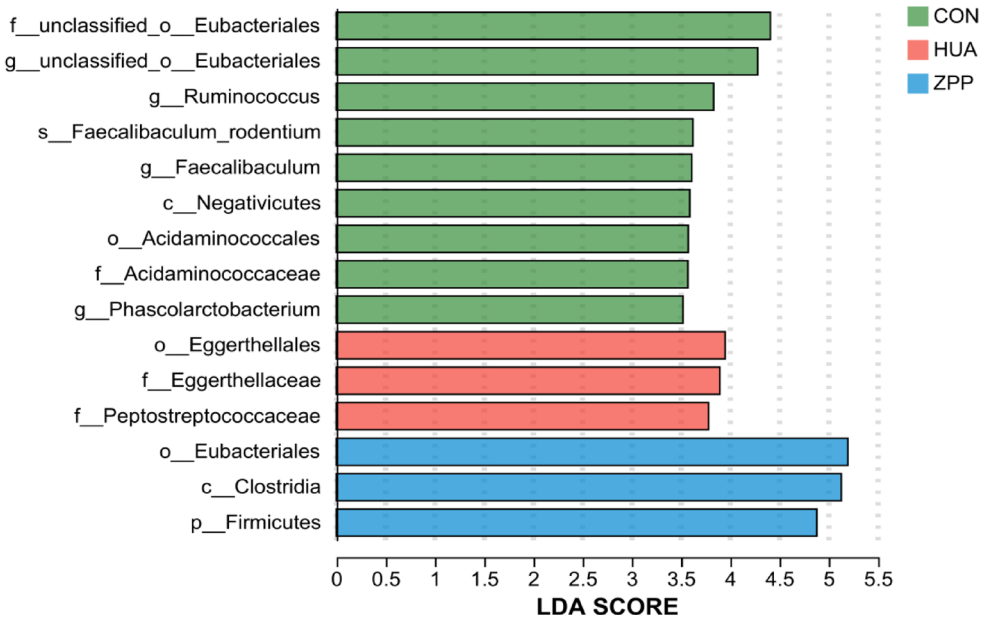

Fig. 7. (**A**) Cladogram of the CON, HUA, and ZPP groups. (**B**) LDA value distribution histogram (LDA > 3.5). (**C**) Circos of species and functional contribution analysis.

C

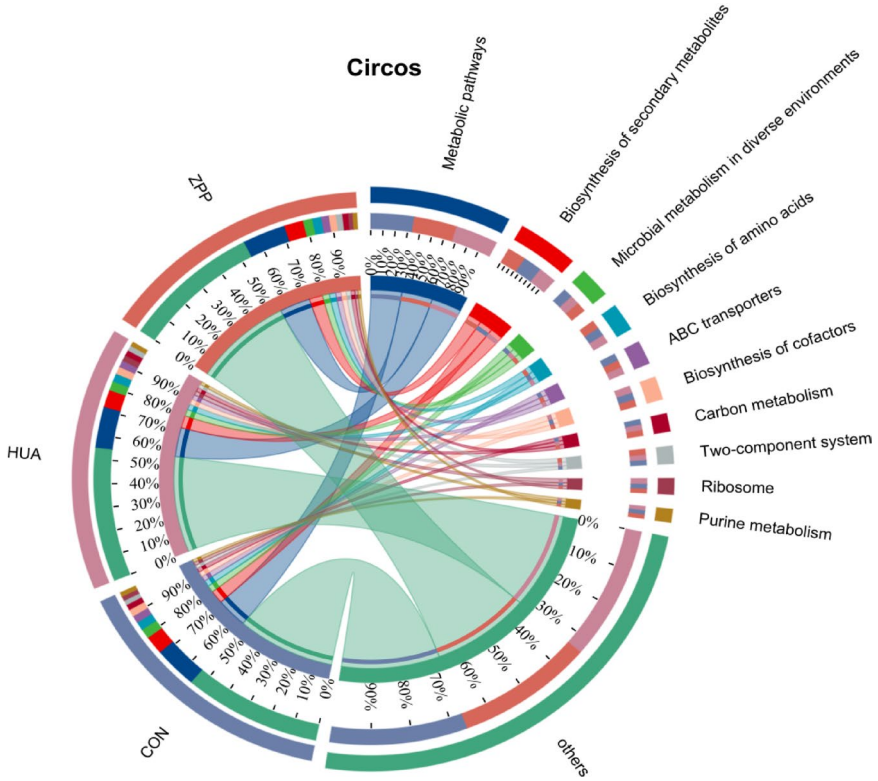

Fig. 7. (continued)

as Metabolic pathways, Biosynthesis of secondary metabolites, Microbial metabolism in diverse environments, Biosynthesis of amino acids, Biosynthesis of cofactors, ABC transporters, Carbon metabolism, Two-component system, Ribosome, and Purine metabolism in hyperuricemia rats (Fig. 7C).

Discussion

Potassium oxonate, as a uricase inhibitor, was widely used to create hyperuricemic rat models[31,32]. Hypoxanthine and adenine serve as biosynthetic precursors of uric acid in the body. Previous studies have reported that adenine supplementation is used to induce hyperuricemia and kidney damage[33,34]. Therefore, the combined use of potassium oxonate, hypoxanthine, and adenine mimics hyperuricemia caused by purine metabolism disorders in humans consuming a high-purine diet, leading to elevated serum uric acid levels, kidney tissue damage, and changes in related indicators. In this study, potassium oxonate, hypoxanthine, and adenine were administered continuously for 21 days, resulting in a steady increase in serum uric acid levels, as well as significant abnormalities in serum Cr and BUN levels, which were related to kidney function. Furthermore, pathological studies found tubular dilatation, tubular epithelial cell edema, interstitial connective tissue hyperplasia, and inflammatory cell infiltration. This suggested that the replication method used in this study for inducing hyperuricemia was successful. We found that ZPP effectively reduced serum uric acid levels in model animals, prevented the increase in serum Cr and BUN levels, and ameliorated renal injury, demonstrating its favorable uric acid-lowering and renal protective effects.

The occurrence and process of hyperuricemia is usually accompanied by abnormal endogenous metabolites[13,14]. To explore the role of ZPP in influencing metabolites, this study determined the changes of differential metabolites and related metabolic pathways in serum by using UPLC-Q-TOF/MS metabolomics technology and identified 23 significantly different relative abundance metabolites in ZPP high-dose group and model groups. Moreover, multiple metabolic pathways were obtained involving purine metabolism, amino acid metabolism, and lipid metabolism, suggesting the potential of ZPP in regulating metabolic pathways effect.

Abnormal purine metabolism is one of the important causes of hyperuricemia[35]. Our study showed that levels of xanthine, deoxyinosine, L-glutamine, and allantoic acid, which involved in purine synthesis and metabolism, were higher in hyperuricemia rats compared to normal rats. This difference was due to the prolonged administration of potassium oxazinate, hypoxanthine, and adenine during the modeling process. The levels of these four metabolites in the ZPP group were closer to those in the normal group, indicating that ZPP could regulate purine metabolism disorders in hyperuricemia rats.

In addition to building proteins, amino acids involved in metabolic processes, including uric acid metabolism. Studies have shown that there a positive correlation between amino acid levels and uric acid levels in the body[36,37]. In this experiment, we also found that serum L-glutamine and L-arginine were elevated in hyperuricemia rats

and returned to normal after ZPP intervention. It was suggested that serum amino acid metabolism markers can be used as diagnostic indicators of hyperuricemia. After ZPP intervention, L-glutamine and L-arginine returned to normal, suggesting that ZPP may alleviate hyperuricemia by regulating the disorder of amino acid metabolism in *vivo* and reducing uric acid production.

Hyperuricemia is widely recognized as a key risk factor for dyslipidemia. Several studies have shown a positive association between serum uric acid levels and lipid profiles in adult populations in China, Italy, and the United States[38–40]. In this study, hyperuricemia rats exhibited abnormalities in various lipid metabolic pathways, including arachidonic acid metabolism, biosynthesis of unsaturated fatty acids, phospholipid metabolism, sphingolipid metabolism, and steroid biosynthesis. Arachidonic acid, a common unsaturated fatty acid, can be converted into various metabolites through three metabolic pathways: cyclooxygenase (COX), lipoxygenase (LOX), and cytochrome P450 (CYP450). These metabolites can trigger different inflammatory reactions[41,42]. Studies have shown that arachidonic acid metabolism is closely related to kidney inflammation, and Leukotriene B4, as a metabolite of arachidonic acid, is considered an inflammatory agent in gout[43,44]. We found elevated levels of arachidonic acid and Leukotriene B4 in the serum of hyperuricemia rats, corresponding to the symptoms of inflammatory cell infiltration observed in renal histopathology. ZPP could ameliorate the abnormalities of arachidonic acid and its metabolites and relieve renal inflammation in hyperuricemia rats, suggesting that ZPP has potential anti-inflammatory and renal protective effects. The phospholipid metabolites LysoPC(20:4), LysoPE(18:0), LysoPC(18:1) and Sphinganine, Sphingosine were also found in the serum of rats with high uric acid anormalities of 1-phosphate, which were consistent with some previous reports[45,46]. After ZPP intervention, these lipid metabolites approached the levels of the blank control group, suggesting that phospholipid and sphingolipid metabolites can be used as diagnostic markers of hyperuricemia. In addition, we found an increase in serum cholesterol and a decrease in its synthetic precursor CE(20:4) in model rats, indicating increased cholesterol synthesis in hyperuricemia. ZPP was able to reverse this situation, suggesting that it may inhibit the steroid biosynthesis pathway.

In recent years, numerous studies have indicated that patients with hyperuricemia suffer from intestinal flora imbalance, and intestinal microorganisms play a significant role in the pathogenesis of hyperuricemia[47,48]. Metagenomics analysis revealed that, at the phylum level, the relative abundance of firmicutes in the gut microbiota of untreated hyperuricemia rats was lower than that of normal rats and rats after ZPP intervention. Meanwhile, compared with the ZPP group, Bacteroidetes were more abundant in hyperuricemia rats. This result was consistent with the reported abnormal ratio of firmicutes to Bacteroidetes when intestinal flora was disturbed in hyperuricemia[49,50]. It has been shown that *Limosilactobacillus reuteri* has the ability to inhibit UA biosynthesis by enhancing gastrointestinal barrier function and promote UA removal by upregulating uric acid transporter[51]. *Ligilactobacillus murinus*, a member of the Lactobacillus genus, a wide range of roles in host intestinal metabolism and immune activity, and its numbers are strongly correlated with intestinal health[52]. In this study, it was found that ZPP increased the relative abundance of two lactobacillus species, *Limosilactobacillus reuteri* and *Ligilactobacillus murinus*, suggesting that ZPP may regulate uric acid metabolism in hyperuricemia rats. *Lachnospiraceae bacterium* and *Oscillospiraceae bacterium*, which are responsible for producing short-chain fatty acids, be negatively correlated with serum uric acid levels[53,54]. Additionally, we identified several probiotics belonging to the phylum Firmicutes, such as *Lachnospiraceae bacterium*, and *Oscillospiraceae bacterium*, whose relative abundances approached those of normal rats after ZPP intervention. The LEfSe analysis revealed that the microorganisms exerting significant effects in the ZPP group were Firmicutes (phylum), Clostridia (class, belonging to Firmicutes), and Eubacteriales (order, belonging to Clostridia). It can be summarized that ZPP primarily reduces serum UA levels in hyperuricemia rats by enhancing the relative abundance of beneficial probiotics within the Firmicutes phylum. Furthermore, the findings from this metagenomics study indicated that ZPP regulatepurine and amino acid metabolism in hyperuricemia rats, aligning with the results obtained from metabolomics analysis.

Conclusion

In summary, this study found that ZPP could reduce serum uric acid levels in hyperuricemia rats and improved renal pathological indexes. Using UPLC-Q-TOF/MS metabolomics techniques, significant alterations in differential metabolites and metabolic pathways were observed in hyperuricemia rats, particularly those involved in purine metabolism, amino acid metabolism, and lipid metabolism. The study found that ZPP was able to ameliorate these metabolic abnormalities, bringing the levels of key metabolites closer to those of normal rats. Additionally, ZPP has also been shown to regulate gut microbiota, specifically by increasing the relative abundance of probiotics within the Firmicutes phylum, which contributed to its uric acid-lowering effects. Overall, these findings indicated that ZPP has potential functionin the prevention and treatment of hyperuricemia, as it addressed metabolic disorders and gut microbiota imbalances associated with the condition.

Data availability

Sequence data that support the findings of this study have been deposited in National Library of Medicine with the primary accession code PRJNA1242895, https://trace.ncbi.nlm.nih.gov/Traces/?view=study&acc=SRP573847. The other data that support the findings of this study are available from the corresponding author, Haixue Kuang, upon reasonable request.

Received: 15 March 2025; Accepted: 25 June 2025
Published online: 07 July 2025

References

1. Mandel, N. S. & Mandel, G. S. Monosodium urate monohydrate, the gout culprit. *J. Am. Chem. Soc.* **98**, 2319–2323 (1976).
2. Dalbeth, N., Gosling, A. L., Gaffo, A. & Abhishek, A. Gout. *Lancet* **397**, 1843–1855 (2021).
3. Barnini, C. et al. Asymptomatic hyperuricemia and the kidney: Lessons from the urrah study. *Metabolites* **15**, 11 (2025).
4. Butler, F., Alghubayshi, A. & Roman, Y. The epidemiology and genetics of hyperuricemia and gout across major racial groups: A literature review and population genetics secondary database analysis. *J. Pers. Med.* **11**, 231 (2021).
5. Choi, H. K. et al. Population impact attributable to modifiable risk factors for hyperuricemia. *Arthritis Rheumatol.* **72**, 157–165 (2020).
6. Aihemaitijiang, S. et al. The association between purine-rich food intake and hyperuricemia: A cross-sectional study in chinese adult residents. *Nutrients* **12**, 3835 (2020).
7. Gliozzi, M., Malara, N., Muscoli, S. & Mollace, V. The treatment of hyperuricemia. *Int. J. Cardiol.* **213**, 23–27 (2016).
8. Fontana, R. J. et al. Allopurinol hepatotoxicity is associated with human leukocyte antigen class I alleles. *Liver Int.* **41**, 1884–1893 (2021).
9. Jansen, T. L., Reinders, M. K., van Roon, E. N. & Brouwers, J. R. Benzbromarone withdrawn from the european market: another case of "absence of evidence is evidence of absence"?. *Clin. Exp. Rheumatol.* **22**, 651 (2004).
10. Wang, Z. et al. Anti-inflammatory and uric acid lowering effects of euodiae fructus on hyperuricemia and gout mice. *Front. Pharmacol.* **15**, 1296075 (2024).
11. Mao, Y., Xu, H. & Xia, P. Ilex cornuta leaves extracts ameliorate hyperuricemia by modulating uric acid transporters. *J. Ethnopharmacol.* **336**, 118618 (2025).
12. Cui, L., Lu, H. & Lee, Y. H. Challenges and emergent solutions for Lc-Ms/Ms based untargeted metabolomics in diseases. *Mass Spectrom. Rev.* **37**, 772–792 (2018).
13. Wu, X. & You, C. The biomarkers discovery of hyperuricemia and gout:proteomics and metabolomics. *PeerJ* **11**, e14554 (2023).
14. Shen, X. et al. Serum metabolomics identifies dysregulated pathways and potential metabolic biomarkers for hyperuricemia and gout. *Arthritis Rheumatol.* **73**, 1738–1748 (2021).
15. Ji, X. et al. Investigating the effects of rare ginsenosides on hyperuricemia and associated sperm damage via nontargeted metabolomics and gut microbiota. *J. Ethnopharmacol.* **332**, 118362 (2024).
16. Wang, Y. et al. Integrating metabolomics with network pharmacology to reveal the mechanism of poria cocos in hyperuricemia treatment. *J. Ethnopharmacol.* **337**, 118977 (2025).
17. Agus, A., Clément, K. & Sokol, H. Gut microbiota-derived metabolites as central regulators in metabolic disorders. *Gut* **70**, 1174–1182 (2021).
18. Fan, Y. & Pedersen, O. Gut microbiota in human metabolic health and disease. *Nat. Rev. Microbiol.* **19**, 55–71 (2021).
19. Wang, Z. et al. Gut microbiota remodeling: A promising therapeutic strategy to confront hyperuricemia and gout. *Front. Cell. Infect. Microbiol.* **12**, 935723 (2022).
20. Kim, N. et al. Genome-resolved metagenomics: A game changer for microbiome medicine. *Exp. Mol. Med.* **56**, 1501–1512 (2024).
21. Wang, D. et al. Comprehensive metabolite profiling of plantaginis semen using ultra high performance liquid chromatography with electrospray ionization quadrupole time-of-flight tandem mass spectrometry coupled with elevated energy technique. *J. Sep. Sci.* **39**, 1842–1852 (2016).
22. Samuelsen, A. B., Lund, I., Djahromi, J., Paulsen, B. S. & Knutsen, S. Structural features and anti-complementary activity of some heteroxylan polysaccharide fractions from the seeds of *Plantago major* L.. *Carbohydr. Polym.* **38**, 133–143 (1999).
23. Beara, I. N. et al. Plantain (Plantago L.) species as novel sources of flavonoid antioxidants. *J. Agric. Food Chem.* **57**, 9268–9273 (2009).
24. Bianco, A., Guiso, M., Passacantilli, P. & Francesconi, A. Iridoid and phenypropanoid glycosides from new sources. *J. Nat. Prod.* **47**, 901–902 (1984).
25. Ahmad, M. S., Ahmad, M. U. & Osman, S. M. A new hydroxyolefinic acid from plantago major seed oil. *Phytochemistry* **19**, 2137–2139 (1980).
26. Yang, F. et al. Lipidomics study of the therapeutic mechanism of plantaginis semen in potassium oxonate-induced hyperuricemia rat. *Bmc Complement. Med. Ther.* **21**, 175 (2021).
27. Liu, T. et al. Plantaginis semen ameliorates hyperuricemia induced by potassium oxonate. *Int. J. Mol. Sci.* **25**, 8548 (2024).
28. Zhao, H. et al. Plantaginis semen polysaccharides ameliorate renal damage through regulating Nlrp3 inflammasome in gouty nephropathy rats. *Food Funct.* **12**, 2543–2553 (2021).
29. Kanehisa, M., Sato, Y., Kawashima, M., Furumichi, M. & Tanabe, M. Kegg as a reference resource for gene and protein annotation. *Nucleic. Acids. Res.* **44**, D457–D462 (2016).
30. Kanehisa, M. & Goto, S. Kegg: Kyoto encyclopedia of genes and genomes. *Nucleic. Acids. Res.* **28**, 27–30 (2000).
31. Liu, H. B. et al. Dispelling dampness, relieving turbidity and dredging collaterals decoction, attenuates potassium oxonate-induced hyperuricemia in rat models. *Drug Des. Devel. Ther.* **17**, 2287–2301 (2023).
32. Hou, S. W. et al. Emodin, a natural anthraquinone, increases uric acid excretion in rats with potassium oxonate-induced hyperuricemia. *Pharmaceuticals* **16**, 789 (2023).
33. Lin, X. et al. Bi Xie Fen Qing Yin decoction alleviates potassium oxonate and adenine induced-hyperuricemic nephropathy in mice by modulating gut microbiota and intestinal metabolites. *Biomed. Pharmacother.* **170**, 116022 (2024).
34. Wang, L. et al. Aqueous extract of phellinus igniarius ameliorates hyperuricemia and renal injury in adenine/potassium oxonate-treated mice. *Biomed. Pharmacother.* **177**, 116859 (2024).
35. Dewulf, J. P., Marie, S. & Nassogne, M. C. Disorders of purine biosynthesis metabolism. *Mol. Genet. Metab.* **136**, 190–198 (2022).
36. Mahbub, M. H. et al. Alteration in plasma free amino acid levels and its association with gout. *Environ. Health Prev.* **22**, 7 (2017).
37. Mahbub, M. H. et al. Association of plasma free amino acids with hyperuricemia in relation to diabetes mellitus, dyslipidemia, hypertension and metabolic syndrome. *Sci. Rep.* **7**, 17616 (2017).
38. Zhang, S., Zhang, Y., Lin, S., Zhang, S. & Qiu, M. Hyperuricemia as a possible risk factor for abnormal lipid metabolism in the chinese population: A cross-sectional study. *Ann. Palliat. Med.* **10**, 11454–11463 (2021).
39. Lippi, G., Montagnana, M., Luca, S. G., Targher, G. & Cesare, G. G. Epidemiological association between uric acid concentration in plasma, lipoprotein(a), and the traditional lipid profile. *Clin. Cardiol.* **33**, E76–E80 (2010).
40. Peng, T. C. et al. Relationship between hyperuricemia and lipid profiles in Us adults. *Biomed. Res. Int.* **2015**, 127596 (2015).
41. Calder, P. C. Marine omega-3 fatty acids and inflammatory processes: Effects, mechanisms and clinical relevance. *Biochim. Biophys. Acta.* **1851**, 469–484 (2015).
42. Yates, C. M., Calder, P. C. & Ed, R. G. Pharmacology and therapeutics of omega-3 polyunsaturated fatty acids in chronic inflammatory disease. *Pharmacol. Ther.* **141**, 272–282 (2014).
43. Wang, T. et al. Arachidonic acid metabolism and kidney inflammation. *Int. J. Mol. Sci.* **20**, 3683 (2019).
44. Rae, S. A., Davidson, E. M. & Smith, M. J. Leukotriene B4, an inflammatory mediator in gout. *Lancet* **2**, 1122–1124 (1982).
45. Sui, X. et al. Protease-activated receptor-2 and phospholipid metabolism analysis in hyperuricemia-induced renal injury. *Mediat. Inflamm.* **2023**, 5007488 (2023).
46. Qin, N. et al. High-throughput untargeted serum metabolomics analysis of hyperuricemia patients by Uplc-Q-Tof/Ms. *Evid. Based Complement Altern. Med.* **2021**, 5524772 (2021).
47. Chu, Y. et al. Metagenomic analysis revealed the potential role of gut microbiome in gout. *Npj Biofilms Microbomes.* **7**, 66 (2021).
48. Yin, H., Liu, N. & Chen, J. The role of the intestine in the development of hyperuricemia. *Front. Immunol.* **13**, 845684 (2022).

49. Deng, S. et al. 16S rrna and metagenomics combined with Uplc-Q/Tof-Ms metabolomics analysis reveals the potential mechanism of radix astragali against hyperuricemia in mice. *Drug Des. Devel. Ther.* **17**, 1371–1386 (2023).
50. Wang, Z. et al. Effects of sporisorium reiliana polysaccharides and phoenix dactylifera monosaccharides on the gut microbiota and serum metabolism in mice with fructose-induced hyperuricemia. *Arch. Microbiol.* **204**, 436 (2022).
51. Hussain, A. et al. Limosilactobacillus reuteri Hcs02–001 attenuates hyperuricemia through gut microbiota-dependent regulation of uric acid biosynthesis and excretion. *Microorganisms* **12**, 637 (2024).
52. Chuandong, Z. et al. Distribution and roles of ligilactobacillus murinus in hosts. *Microbiol. Res.* **282**, 127648 (2024).
53. Sheng, S. et al. Structural and functional alterations of gut microbiota in males with hyperuricemia and high levels of liver enzymes. *Front. Med.* **8**, 779994 (2021).
54. Zhang, W. et al. Variation of serum uric acid is associated with gut microbiota in patients with diabetes mellitus. *Front. Cell. Infect. Microbiol.* **11**, 761757 (2021).

Author contributions

Conceptualization, H.K. and D.W.; methodology, J.N.; software, D.W. and J.N.; validation, D.W. and J.N.; formal analysis, H.W.; investigation, J.H. and H.W.; resources, D.W.; data curation, J.H.; writing—original draft preparation, D.W. and J.N.; writing—review and editing, H.K.; visualization, J.H.; supervision, H.K. and D.W.; project administration, H.K. and D.W.

Funding

Science and Technology Research Key Project of Quzhou. (2022K109).

Declarations

Competing interest

The authors declare no competing interests.

Ethical approval

The study was approved by the Experimental Animal Ethics Committee of the Academic Committee of Tianjin University of Chinese Medicine (project identification code: TCM-LAEC2022260n1453). All methods were carried out in accordance with relevant guidelines and regulations, and all animal studies complied with relevant ethical regulations on animal testing and research and followed by the ARRIVE guidelines (https://arriveguidelines.org).

Additional information

Supplementary Information The online version contains supplementary material available at https://doi.org/10.1038/s41598-025-09048-1.

Correspondence and requests for materials should be addressed to H.K.